Organic Electronics 13 (2012) 850–855

Contents lists available at SciVerse ScienceDirect

Organic Electronics

journal homepage: www.elsevier.com/locate/orgel

Charge injection and transport studies of poly(2,7-carbazole) copolymer PCDTBT and their relationship to solar cell performance

Kevin K.H. Chan [a], S.W. Tsang [b], Harrison K.H. Lee [a], Franky So [b], S.K. So [a,*]

[a] Department of Physics and Centre for Advanced Luminescence Materials, Hong Kong Baptist University, Kowloon Tong, Hong Kong, China
[b] Department of Materials Science and Engineering, University of Florida, Gainesville, FL 32611-6400, USA

ARTICLE INFO

Article history:
Received 15 November 2011
Received in revised form 5 January 2012
Accepted 29 January 2012
Available online 13 February 2012

Keywords:
PCDTBT
Charge transport properties
Dark-injection space-charge-limited current
Carrier mobility
Energetic disorder

ABSTRACT

The charge injection and transport properties of a high performance semiconducting polymer for organic photovoltaic (OPV) applications, poly[*N*-9″-hepta-decanyl-2,7-carbazole-alt-5,5-(4′,7′-di-2-thienyl-2′,1′,3′-benzothiadiazole)] (PCDTBT), are investigated by time-of-flight (TOF) and dark-injection space-charge-limited current (DI-SCLC) techniques. OPV cells employing PCDTBT are known to possess power conversion efficiency (PCE) exceeding 6% [1,2]. While TOF probes only the hole mobilities of a thick film, DI-SCLC is shown to be useful down to a sample thickness of ~200 nm, which is comparable to thicknesses used in OPV cells. We show that for pristine PCDTBT, the hole mobilities for both thick used in TOF and thin films for DI-SCLC are essentially the same, and they are in the range of $0.4–3.0 \times 10^{-4}$ cm^2/Vs at room temperature. Both poly(3,4-ethylene dioxythioplene) doped with poly(strenesulfonate) (PEDOT:PSS) and molybdenum (VI) oxide (MoO_3) form quasi-Ohmic contacts to PCDTBT with better hole injection from MoO_3. Furthermore, the Gaussian Disorder Model (GDM) was employed to analyze the hopping transport of PCDTBT thin films. We show that PCDTBT possesses a relatively large energetic disorder (σ) of ~129 meV, which is significantly higher than the σ of poly(3-hexylthiophene) (P3HT) processed under similar conditions. The correlation between σ and OPV device performance is addressed.

1. Introduction

Currently, semi-conducting polymers have received world-wide attentions. Organic light-emitting diodes, organic thin film transistor, and organic photovoltaic (OPV) cells are some of the applications based on semi-conducting polymers [3–5]. Among these applications, OPV cells are appealing as they convert solar energy to electricity which has high potential for developing low-cost photovoltaic technology. Recently, 8% power conversion efficiency (PCE) has been already reached with low bandgap co-polymers [6]. In order to further improve the OPV cell efficiency, the operating mechanisms need to be understood.

It has been widely discussed that charge transport properties of OPV materials play a key role in determining the device performance. Several techniques are commonly used to investigate the transport properties of semi-conducting polymers, including time-of-flight (TOF), thin film transistor, admittance spectroscopy, and dark-injection space-charge-limited current (DI-SCLC) [7–12]. In this contribution, a classic technique, DI-SCLC, is employed to investigate the carrier transport properties of a novel semi-conducting polymer, poly[*N*-9″-hepta-decanyl-2,7-carbazole-alt-5,5-(4′,7′-di-2-thienyl-2′,1′,3′-benzothiadiazole)] (PCDTBT) for OPV applications. The basic principle of DI-SCLC is well-known [7,11–13]. Briefly, the active material is investigated in a sandwiched structure of anode/organic/cathode. A step voltage is then applied to induce a temporal current response. If the injection contact is Ohmic, the carrier mobility (μ) can be determined from

* Corresponding author. Tel.: +86 852 3411 7038; fax: +86 852 3411 5813.
E-mail address: skso@hkbu.edu.hk (S.K. So).

1566-1199/$ - see front matter © 2012 Elsevier B.V. All rights reserved.
doi:10.1016/j.orgel.2012.01.030

the characteristic features in the transient current. Therefore a good electrical contact is necessary for DI-SCLC experiments. For PCDTBT, we show that both poly(3,4-ethylenedioxythioplene) doped with poly(strenesulfonate) (PEDOT:PSS) and molybdenum (VI) oxide (MoO_3) can form quasi-Ohmic contacts to PCDTBT, despite its relatively low-lying HOMO of ~ -5.5 eV [14]. Using these two materials as the hole injection contacts, very well-defined DI-SCLC signals can be obtained even for thin films with a thickness down to 200 nm. The extracted hole mobilities are in the range of $0.4–1 \times 10^{-4}$ cm^2/Vs. In addition, temperature dependent experiments were carried out to extract the energetic disorder (σ) of PCDTBT. It turns out σ for PCDTBT is $\sim$129 meV, which is significantly larger than that for P3HT ($\sigma \sim 80$ meV). The implications of large energetic disorders in OPV device parameters will be discussed.

2. Experimental details

PCDTBT was purchased from Lum. Tech. (LT-S948). Its chemical structure and highest occupied molecular orbital (HOMO) [14] were shown in Fig. 1. For comparison, we also show the HOMO level of poly(3-hexythiophene) (P3HT), another popular OPV polymer. The sample for DI-SCLC experiments had a general structure of anode/hole injection layer (HIL)/PCDTBT/cathode. The same sample was also used for current–voltage (J–V) measurements. Pre-patterned indium-tin-oxide (ITO) on glass was used as the substrate. PEDOT:PSS (Clevio P VP Al 4083, H.C. Starck GmbH) and MoO_3 (99.998%, Strem Chemical, Inc.) were chosen as the HIL. The work functions of HILs were shown in Fig. 1c [15–17]. For devices with a PEDOT:PSS anode, a water solution of PEDOT:PSS was spin-coated on ITO. The layer was then annealed at 150 °C for 30 min. The resulting PEDOT:PSS layer had a thickness of 90 nm. For MoO_3 anode, the oxide layer (20 nm) was coated on ITO by thermal evaporation under high vacuum condition. The thicknesses of the HILs have been optimized with respect to DI-SCLC measurements. The coating rate was about 0.2–0.3 Å/s. Before deposition, PCDTBT was first dissolved in chloroform with a concentration of 20 mg/ml and stirred for 16 h at 70 °C inside a nitrogen filled glove box. The PCDTBT solution was then filtered, and spin-coated on the HIL with a speed 600 rpm for 30 s. Subsequently, all samples were naturally dried inside a glove box. The resulting PCDTBT had a thickness of 200–220 nm. Finally, 100 nm of gold (Au) was thermally evaporated on PCDTBT. The Au cathode served as a high work function cathode to prevent electron injection. For TOF measurements, the sample structure of ITO/PCDTBT (3.5 μm)/Al (15 nm) was used. A thick PCDTBT layer was fabricated by drop-casting. The film was naturally dried inside a glove box for about 18 h. A semitransparent Al layer was then deposited on PCDTBT. The thicknesses of the films were measured by a pofilometer (Veeco, Dektak 150). After fabrication, the samples were placed inside a cryostat in vacuum. For DI-SCLC measurement, a rectangular voltage pulse from a pulse generator (HP, Model 241B) was used to inject holes into the sample. The DI-SCLC transient was captured by measuring the voltage across a current sensing resistor (connected in series with the sample). J–V measurements were carried out with a source-measure-unit (SMU) (Keithley Instruments Inc., Model 236). For TOF, a Nd:YAG laser ($\lambda = 532$ nm) was incident through the Al semi-transparent electrode to generate free charges inside PCDTBT. A digital oscilloscope was used to capture the TOF transient in the similar manner as DI-SCLC experiments.

3. Results and discussion

Fig. 2 shows the TOF transient of a thick film of PCDTBT at room temperature under an electric field strength $F = 571$ kV/cm. The signal is quite dispersive; nevertheless the hole transit time (τ) can be determined from a log–log plot (inset of Fig. 2) and the hole mobility (μ_{TOF}) can be calculated by [7,8]:

$$\mu_{TOF} = \frac{d^2}{\tau \cdot V_{applied}}, \quad (1)$$

where d and $V_{applied}$ are the sample thickness and applied voltage across the sample, respectively. In Fig. 3, the extracted TOF field-dependent hole mobilities (filled squares)

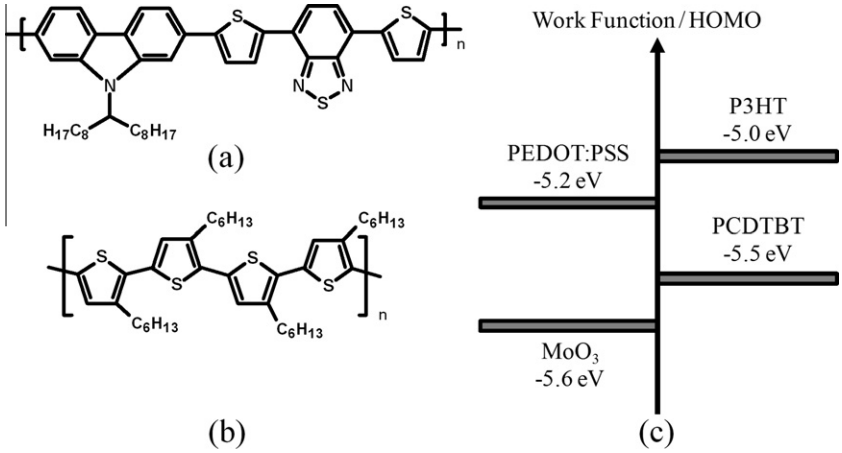

Fig. 1. Chemical structures of (a) PCDTBT and (b) P3HT. (c) Work functions of different hole injection layers and HOMO level of OPV polymers.

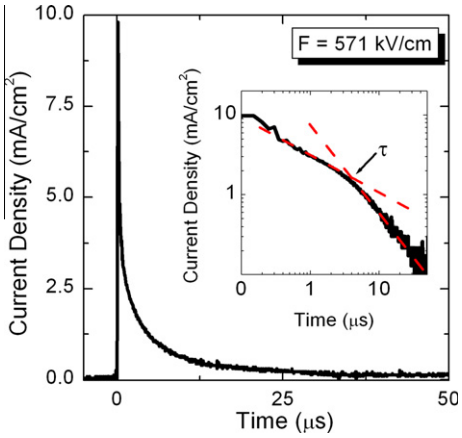

Fig. 2. A typical TOF signal for PCDTBT. The sample has a structure of ITO/PCDTBT (3.5 μm)/Al. A Nd:YAG laser with a wavelength of 532 nm was used as the excitation laser for free carrier generation. The inset shows a log–log plot of the TOF signal from which the hole transit time can be extracted.

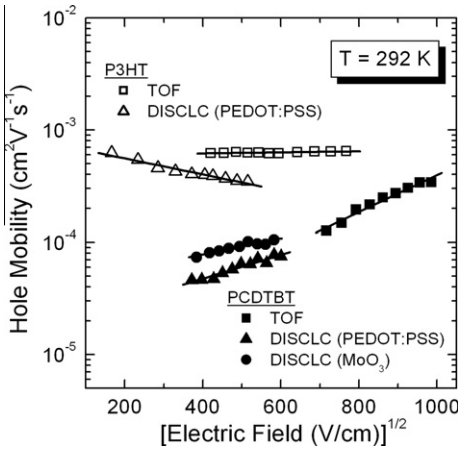

Fig. 3. Hole mobilities of PCDTBT extracted from TOF (filled squares), and DISCLC. For DISCLC, the samples have the structures of either ITO/PEDOT:PSS/PCDTBT (222 nm)/Au (filled triangles) or ITO/MoO_3 (20 nm)/PCDTBT (211 nm)/Au (filled circles). For comparison, the hole mobilities of another popular polymer, P3HT, are also shown (unfilled symbols).

are in the range between 1 and 3×10^{-4} cm^2/Vs under a field range of 0.5–1 MV/cm. In addition, the mobility follows the Poole–Frenkel model with $\mu = \mu_0 \exp(0.89\beta\sqrt{F})$, where β is the Poole–Frenkel slope, and μ_0 is the zero-field mobility, respectively. $\beta = 1.85 \times 10^{-3}$ $(V/cm)^{-1/2}$ and $\mu_0 = 8.89 \times 10^{-6}$ cm^2/Vs can be obtained from the slope and y-intercept of the fitting straight line of the mobility, respectively.

DI-SCLC was chosen for measuring the hole transporting properties in PCDTBT thin films (200–220 nm thick). Fig. 4 shows the DI-SCLC transients of PCDTBT under different biases using PEDOT:PSS (left panel) and MoO_3 (right panel) as HILs. The DI-SCLC transients exhibit the characteristic signatures of classic DI-SCLC signals. For each transient, a distinct hole transit time (τ_{DI}) can be extracted. These observations can only be obtained if the sample

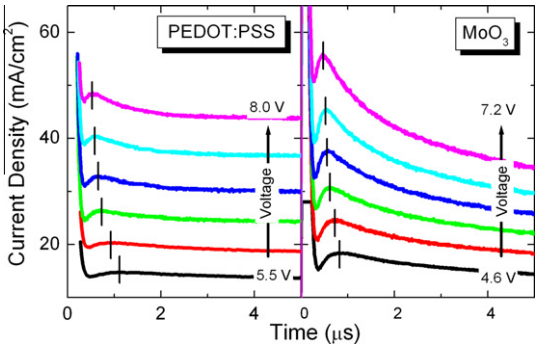

Fig. 4. A sequence of DISCLC signals using (a) PEDOT:PSS, and (b) MoO_3 as the hole injection layers. The carrier transit times are marked with vertical bars.

obeys the following conditions: (i) quasi-Ohmic contact between HIL and organic layer and (ii) unipolar carrier injection. As a result, the hole mobility (μ_{DI}) can be calculated as follows [7,11–13]:

$$\mu_{DI} = \frac{0.787 \cdot d^2}{\tau_{DI} \cdot (V_{applied} - V_{bi})}, \quad (2)$$

where V_{bi} is the built-in voltage, which is an important factor for thin film measurements. In our data analysis, we adopt V_{bi} as the difference between the work functions of the HIL and the cathode [18,19]. The extracted hole mobilities from DI-SCLC are shown alongside (filled triangles and circles) with the TOF data in Fig. 3. The extracted mobilities from DI-SCLC are in good agreement to those determined from TOF technique. The slightly difference between the mobilities of MoO_3 and PEDOT:PSS is attributed to the hole injection barrier at the HIL/PCDTBT contact, which will be discussed below. For comparison, the hole mobilities of P3HT are shown in Fig. 3. Similarly the extracted mobilities of P3HT are also in good agreement between the two techniques.

Fig. 5, top-panel, shows the J–V data of PCDTBT thin films at room temperature with PEDOT:PSS and MoO_3 as HILs. The solid line is the simulated J–V characteristics based on the space-charge-limited current (J_{SCL}) for a trap-free organic material under Ohmic contact [20]:

$$J_{SCL} = \frac{9}{8}\mu_0\varepsilon_0\varepsilon_r \times \exp\left(0.89\beta\sqrt{\frac{V_{applied} - V_{bi}}{d}}\right)\frac{(V_{applied} - V_{bi})^2}{d^3}, \quad (3)$$

where ε_0 is the absolute permittivity, $\varepsilon_r = 3$ is the dielectric constant for the organic material. In computing J_{SCL}, we adopted values of β and μ_0 extract from the TOF data in Fig. 3. J_{SCL} represents the maximum possible hole current that can be sustained by the sample. The ratio between the measured current ($J_{measured}$) and J_{SCL} defines the injection efficiency ($\eta_{INJ} = J_{measured}/J_{SCL}$) and this ratio is shown in the bottom panel of Fig. 5. The dashed line shows $\eta_{INJ} = 100\%$ in case of Ohmic contact injection. From the top panel of Fig. 5, at the high field region ($F > 250$ kV/cm), the $J_{measured}$ of PCDTBT for both HILs are close to the

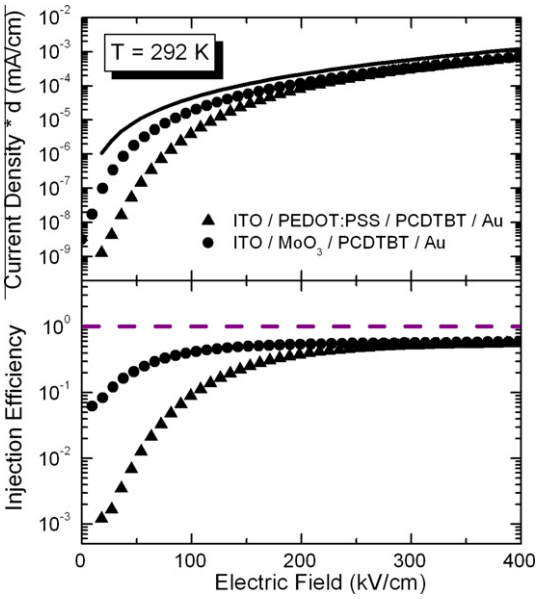

Fig. 5. (a) Top panel: current–voltage curves of samples with a structure of ITO/PEDOT:PSS/PCDTBT (222 nm)/Au (filled triangles) and ITO/MoO_3 (20 nm)/PCDTBT (211 nm)/Au (filled circles). The solid line is the theoretical SCLC current. (b) Bottom panel: hole injection efficiencies of PEDOT:PSS and MoO_3.

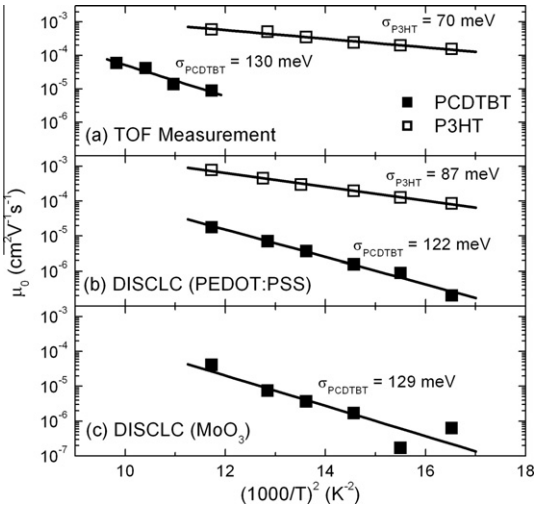

Fig. 6. Zero field mobilities of PCDTBT versus the reciprocal of the square of temperature extracted from TOF or DISCLC. The solid lines are the best linear fits to the data. The energetic disorder can be extracted from the slopes of the fits. For comparison, similar data for P3HT are also shown here.

J_{SCL}. At the low field region ($F < 250$ kV/cm), the contact of MoO_3/PCDTBT is better than PEDOT:PSS. For example, η_{INJ} of PEDOT:PSS/PCDTBT is nearly one order of magnitude lower than that of MoO_3/PCDTBT at $F = 100$ kV/cm. The difference is even more pronounced at lower field strengths. The result is reasonable, assuming that interfacial dipoles are negligible, a larger hole injection barrier (0.3 eV) is formed with the lower work function PEDOT:PSS as the HIL, while the injection barrier is negligible in the case of MoO_3 (Fig. 1c).

In order to investigate the disorder properties of the two materials, temperature dependent measurements were performed for both TOF and DI-SCLC experiments. The transport data were then analyzed by the Gaussian Disorder Model (GDM) [21]. In the GDM, the carriers transport through a disordered molecular material by hopping through Gaussian distributed density-of-states. The model can be summarized by the following equation [21]:

$$\mu(F,T) = \mu_\infty \exp\left[-\left(\frac{2\sigma}{3kT}\right)^2\right] \exp\left(\beta F^{\frac{1}{2}}\right), \quad (4)$$

where μ_∞ is the high-temperature limit of the mobility, k is the Boltzmann constant and T is the absolute temperature. σ is the energetic disorder, which is defined as half of full-width-half-maximum (FWHM) of the Gaussian distribution of energy states for the transport sites. By plotting $\mu(0,T) = \mu_0(T)$ versus $1/T^2$ (Fig. 6), one can determine σ from the slope of the fitting straight line. Fig. 6 summarizes the resulting plots from TOF and DI-SCLC measurements. Two separated panels (Fig. 6b and c) are used to indicate results for DI-SCLC with the two different HILs. For comparison, we also show temperature dependent transport data for P3HT in Fig. 6a and b. The extracted energetic disorder for PCDTBT, σ_{PCDTBT}, is generally agreeable to each other, and is in the range between 122 and 130 meV. In contrast, the energetic disorder for P3HT, σ_{P3HT}, is only about 87 meV. Nano-scale structures are known to have large influence on the energetic disorder of a disordered molecular solid. Generally, an increase in ordering reduces σ. As P3HT is known to form nano-crystalline domains [22], σ is expected to be smaller than PCDTBT that is known to be amorphous [23]. Our experimental results on σ are consistent with the nano-scale structures of P3HT and PCDTBT.

To inspect the OPV properties of the PCDTBT polymer, we fabricated OPV devices using a bulk heterojunction (BHJ) blend consisting of PCDTBT as the donor polymer and [6,6]-phenyl C71 butyric acid methyl ester ($PC_{71}BM$) as the acceptor. Briefly, PCDTBT and $PC_{71}BM$, in a weight percentage of 1:2, were dissolved in chloroform. Subsequently, the solution was spin-coated on a PEDOT:PSS (40 nm thick) anode. The resulting BHJ film has a thickness of about 70–80 nm. After drying, a thin layer of LiF (1 nm), followed by Al were coated on the BHJ film to define the cathode in vacuum. The active area of a cell is 4.3 mm^2. Table 1 and Fig. 7 summarize the device performances of the PCDTBT:$PC_{71}BM$ OPV cell. The device has an open-circuit voltage (V_{OC}) = 0.9 V, short circuit current density (J_{SC}) = 10.2 mA/cm^2, fill-factor (FF) = 59%, and an overall PCE of 5.48%. The device performances are generally comparable to those reported in literatures [1,2]. For comparison, we also show in Table 1 and Fig. 7 the device performances of an OPV cell employing a BHJ blend of P3HT:$PC_{61}BM$ (1:1) fabricated under similar conditions. We note that, with the exception of the *FF*, the PCD TBT:$PC_{71}BM$ cell is in every respect superior to those of the P3HT:PCBM cell.

Table 1
Transport parameters of PCDTBT and P3HT based on DI-SCLC, and their corresponding OPV performance.

Polymer	μ at 160 kV/cm (cm^2/Vs)	σ (meV)	V_{OC} (V)	J_{SC} (mA/cm^2)	*FF* (%)	PCE (%)
PCDTBT	8×10^{-5}	129	0.9	10.2	59	5.48
P3HT	4×10^{-4}	87	0.6	7.5	67	3.04

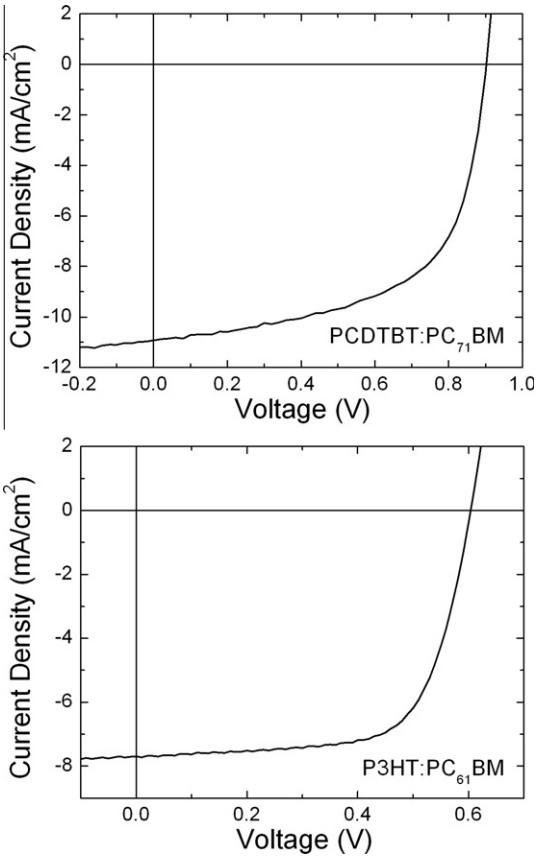

Fig. 7. *J–V* characteristics of PCDTBT based (top panel) and P3HT based (bottom panel) OPV cells under illumination.

Two correlations have been found between the transport data and the PV device performances. First, we comment on V_{OC}. It has been argued that the energetic disorder is related to the OPV performance [24–26]. More recently, it has been shown analytically that V_{OC} and the energetic disorder of the charge transport medium at a fixed temperature T are related by [27]:

$$eV_{OC} = \left(E_{HOMO,D} - E_{LUMO,A} - \sigma^2/kT\right) + kT \ln\left(\frac{G}{\gamma N_h N_e}\right) \qquad (5)$$

In Eq. (5), the first term in parenthesis represents the effective energy gap of the BHJ (E_g^{eff}), which is the difference in energy between the HOMO level of the donor ($E_{HOMO,D}$) and the LUMO level ($E_{LUMO,A}$) of the acceptor, corrected by a term (i.e. $-\sigma^2$/kT) which is related to the energetic disorder. The second term in Eq. (5) represents the loss in V_{OC} arising from recombination loss, which is controlled by the generation rate (G), the recombination constant rate coefficient (γ), and the effective densities for states for holes (N_h) and electrons (N_e). Assuming σ is the only variable in Eq. (5), if σ_{PCDTBT} can be improved from 129 meV to about 87 meV (similar to σ_{P3HT}), the V_{OC} of PCDTBT-based OPV cells can be substantially increased by 0.28 V. Using the data in Table 1, V_{OC} for the PCDTBT cell can be increased to 1.18 V by solely improving the energetic disorder. Second, computer simulations in Ref. [27] show that the fill factor increases when σ decreases. This is attributed to the reduction in γ [24–26,28]. According to the determined σ_{PCDTBT} and σ_{P3HT} in this contribution, we expect that the *FF* of PCDTBT-based OPV cells (FF_{PCDTBT}) should be smaller than P3HT-based OPV cells (FF_{P3HT}). From Fig. 7 and Table 1, we see that FF_{PCDTBT} = 59% and is indeed smaller than FF_{P3HT} = 67%, those values are also consistent with literatures reported [1,2,29,30]. It is suggested that the reduction in the energetic disorder of the material is a viable route for achieving a high PCE.

4. Conclusion

The charge injection and transport properties of PCDTBT films have been investigated by DI-SCLC (200–220 nm) and TOF (3.5 μm). The extracted mobilities from these two techniques are in good agreement. For DI-SCLC, both MoO_3 and PEDOT:PSS form quasi Ohmic contacts to PCDTBT; however, MoO_3 acts as a better HIL since the injection efficiency of MoO_3/PCDTBT is higher at the low field region (F < 250 kV/cm). In addition, the energetic disorder of PCDTBT (σ_{PCDTBT}) determined from temperature dependent measurements is about 129 meV, which is significantly larger than the energetic disorders of P3HT ($\sigma_{P3HT} \sim 80$ meV). With a smaller energetic disorder, we expect both the open-circuit voltage and the fill-factor of an OPV cell can be enhanced, leading to a higher power conversion efficiency.

Acknowledgments

Supports of this research by the Research Committee of Hong Kong Baptist University under Grant No. FRG2/10-11/090, a HKBU SDF Grant # 03-17-023, and the Research Grant Council of Hong Kong under Grant No. HKBU210608E, are gratefully acknowledged. The work was also partially supported by a grant from the Research Grants Council of the Hong Kong Special Administrative Region, China (Project No. [T23-713/11]).

References

[1] S. Alem, T. Chu, S.C. Tse, S. Wakim, J. Lu, R. Movileanu, Y. Tao, F. Bélanger, D. Désilets, S. Beaupré, M. Leclerc, S. Rodman, D. Waller, R. Gaudiana, Org. Electron. 12 (2011) 1788.
[2] S.H. Park, A. Roy, S. Beaupré, S. Cho, N. Coates, J.S. Moon, D. Moses, M. Leclerc, K. Lee, A.J. Heeger, Nat. Photonics 3 (2009) 297.
[3] J.H. Burroughes, D.D.C. Bradley, A.R. Brown, R.N. Marks, K. Mackay, R.H. Friend, P.L. Burns, A.B. Holmes, Nature (London) 347 (1990) 539.
[4] Y.Q. Liu, Y.G. Wen, Adv. Mater. 22 (2010) 1331.
[5] W. Cai, X. Gong, Y. Cao, Sol. Energy Mater. Sol. Cells 94 (2010) 114.
[6] H.Y. Chen, J. Hou, S. Zhang, Y. Liang, G. Yang, Y. Yang, L. Yu, Y. Wu, G. Li, Nat. Photonics 3 (2009) 649.

[7] S.C. Tse, C.H. Cheung, S.K. So, Organic electronics: materials, processing devices and application, in: F. So (Ed.), CRC Press, Francis and Taylor, 2010. Chapter 3.
[8] K.K. Tsung, S.K. So, Org. Electron. 10 (2009) 661.
[9] Cyrus Y.H. Chan, C.M. Chow, S.K. So, Org. Electron. 12 (2011) 1454.
[10] K.H. Chan, S.K. So, J. Photon. Energy 1 (2011) 011112.
[11] C.H. Cheung, K.C. Kwok, S.C. Tse, S.K. So, J. Appl. Phys. 103 (2008) 093705.
[12] C.H. Cheung, W.J. Song, S.K. So, Org. Electron. 11 (2010) 89.
[13] M.A. Lampert, P. Mark, Current Injection in Solids, Academic, New York, 1970.
[14] N. Blouin, A. Michaud, D. Gendron, S. Wakim, E. Blair, R. Neagu-Plesu, M. Belletête, G. Durocher, Y. Tao, M. Leclerc, J. Am. Chem. Soc. 130 (2008) 732.
[15] Y. Kinoshita, R. Takenaka, H. Murata, Appl. Phys. Lett. 92 (2008) 243309.
[16] Irfan, H. Ding, Y. Gao, C. Small, D.Y. Kim, J. Subbiah, F. So, Appl. Phys. Lett. 96 (2010) 243307.
[17] J. Meyer, R. Khalandovsky, P. Görrn, A. Kahn, Adv. Mater. 23 (2011) 70.
[18] G.G. Malliaras, J.R. Salem, P.J. Brock, J.C. Scott, J. Appl. Phys. 84 (1998) 1583.
[19] T.M. Brown, J.S. Kim, R.H. Friend, F. Cacialli, R. Daik, W.J. Feast, Appl. Phys. Lett. 75 (1999) 1679.
[20] P.N. Murgatroyd, J. Phys. D 3 (1970) 151.
[21] H. Bässler, Phys. Status Solidi B 175 (1993) 15.
[22] T. Erb, U. Zhokhavets, G. Gobsch, S. Raleva, B. Stühn, P. Schilinsky, C. Waldauf, C.J. Brabec, Adv. Funct. Mater. 15 (2005) 1193.
[23] See e.g., Fig. S7 in Supplementary Information of Ref. [2].
[24] M. Tachiya, K. Seki, Phys. Rev. B 82 (2010) 085201.
[25] C.G. Shuttle, B. O'Regan, A.M. Ballantyne, J. Nelson, D.D.C. Bradley, J.R. Durrant, Phys. Rev. B 78 (2008) 113201.
[26] J. Nelson, Phys. Rev. B 67 (2003) 155209.
[27] J.C. Blakesley, D. Neher, Phys. Rev. B 84 (2011) 075210.
[28] S. Chen, K.R. Choudhury, J. Subbiah, C.M. Amb, J.R. Reynods, F. So, Adv. Eng. Mater. 1 (2011) 963.
[29] G. Li, V. Shrotriya, J. Huang, Y. Yao, T. Moriarty, K. Emery, Y. Yang, Nat. Mater. 4 (2005) 864.
[30] T. Xiao, W. Cui, J. Anderegg, J. Shinar, R. Shinar, Org. Electron. 12 (2011) 257.